ISTITUTO NAZIONALE DI FISICA NUCLEARE - ISTITUTO NAZIONALE DI FISICA NUCLEARE - ISTITUTO NAZIONALE DI FISICA NUCLEARE - ISTITUTO NAZIONALE DI FISICA NUCLEARE - ISTITUTO NAZIONALE DI FISICA NUCLEARE - ISTITUTO NAZIONALE DI FISICA NUCLEARE - ISTITUTO NAZIONALE DI

Laboratori Nazionali di Frascati

IT8900543

INFN - LNF- 89/044(R)
28 Giugno 1989

M. Barone, A. Cattoni, C. Sanelli:

SUPERCONDUCTING WIGGLER FOR ADONE: FIRST TESTS AND RESULTS

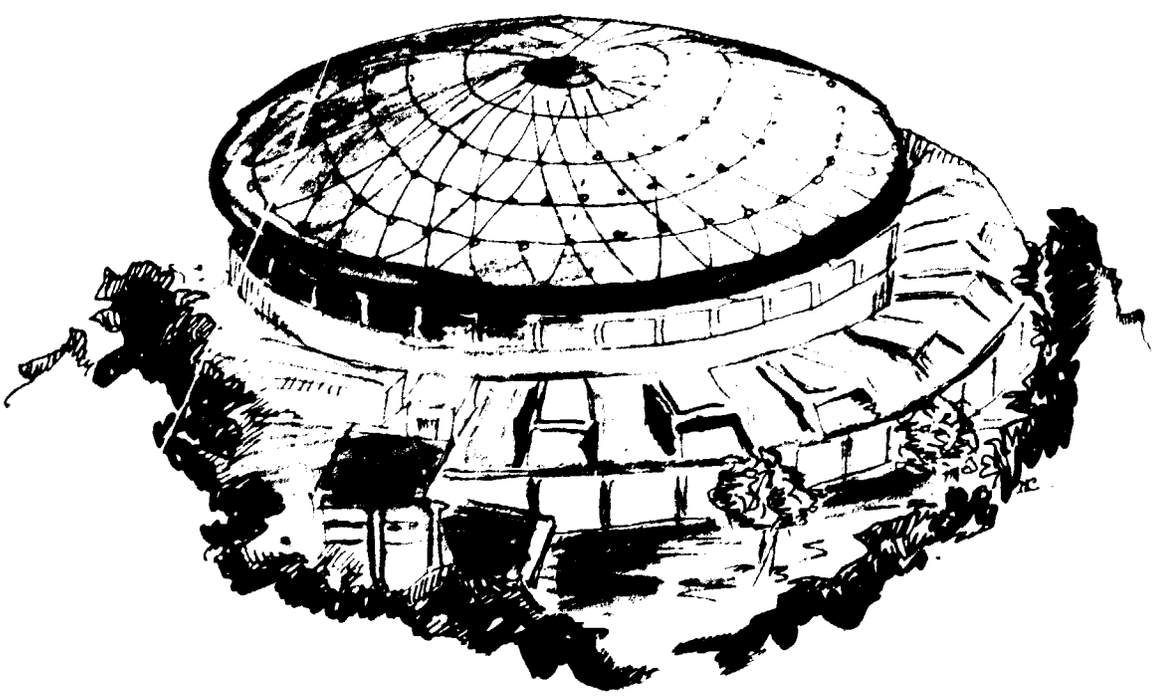

Servizio Documentazione
dei Laboratori Nazionali di Frascati
P.O. Box, 13 - 00044 Frascati (Italy)

INFN - Laboratori Nazionali di Frascati
Servizio Documentazione

LNF- 89/044(R)
28 Giugno 1989

SUPERCONDUCTING WIGGLER FOR ADONE: FIRST TESTS AND RESULTS

M. Barone, A. Cattoni, C. Sanelli
INFN - Laboratori Nazionali di Frascati, P.O.Box 13, 00044 Frascati (Italy)

ABSTRACT

A superconducting wiggler magnet has been successfully tested at ANSALDO COMPONENTI works. The design field of 6 Tesla has been reached after limited training. The field of 6.025 ± 0.003 Tesla has been measured by means of a flip coil connected to an integrating magnetometer. Field profile measurements were made at 5.0, 5.75 and 6.025 Tesla, during which time, the magnet showed high stability. The overall cryogenic losses have been measured and they are consistent with the computed ones.

1. - WIGGLER BASIC CHARACTERISTICS

A superconducting wiggler, to be used as an insertion device in the existing storage ring Adone, has been designed at Laboratori Nazionali INFN, Frascati, and built by Ansaldo Componenti-Genova.

The aim of this facility is to shift the "universal" spectral curve of the synchrotron radiation from the Adone bending magnets towards higher energy photons. At an electron beam energy of 1.5 GeV (B bending = 1 Tesla) and for a circulating beam of 100 mA, the present photon flux at 1.5 KeV (critical energy) is about $2.4*10^{12}$ photons/s mrad 0.1% bw. (see Fig. 1). The same flux can be obtained at 9 KeV from the 6 Tesla magnetic field of the wiggler.

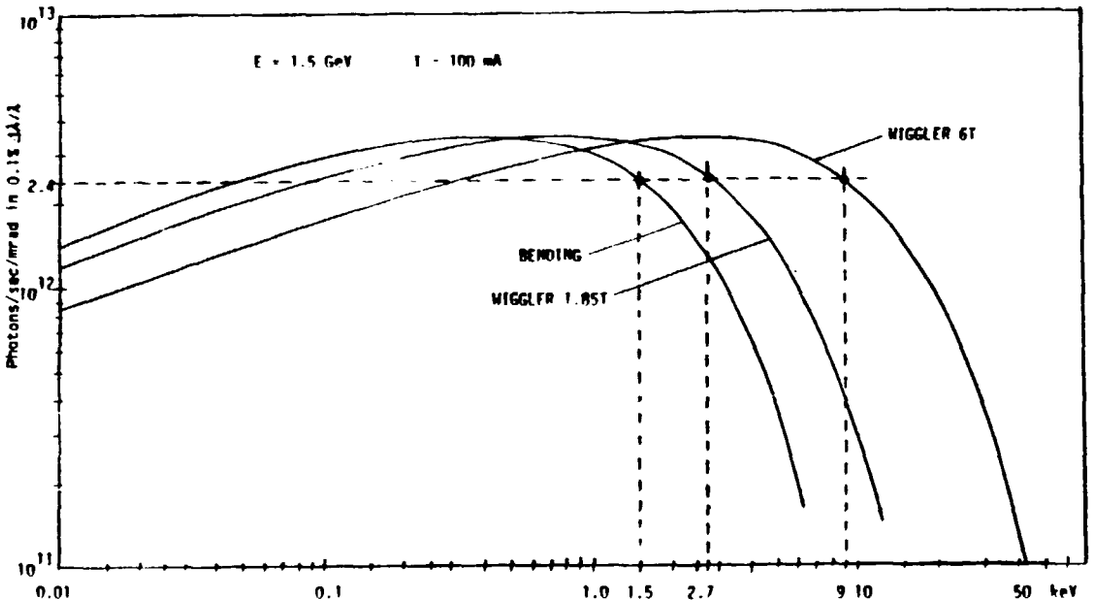

FIG. 1

An important aspect is the structure of the synchrotron light source to be obtained, namely its horizontal and vertical phase space distributions (Fig. 2). The source created by a wiggler has a structure (in both planes) whose complexity depends on number of the "wiggles" (electron orbit oscillations in the wiggler).

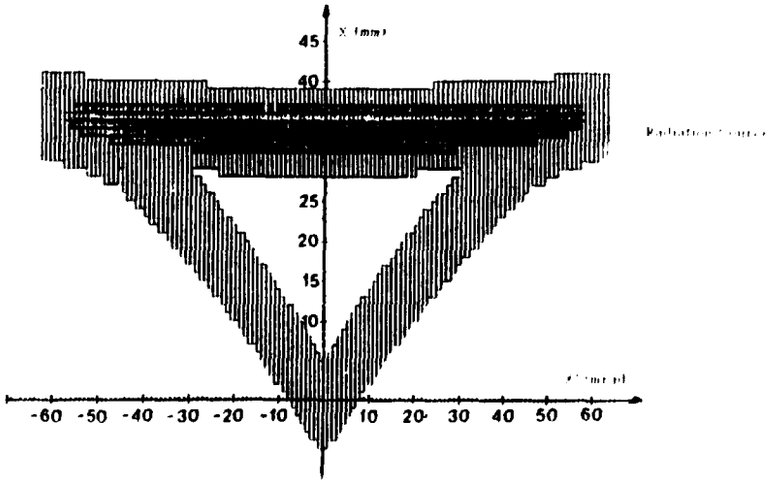

FIG. 2

To be compatible with the storage ring optics, the wiggler must also fulfill the following conditions:

1) $\int Bz\, ds \sim 0$ (the first integral of the vertical field component should vanish).
2) The orbit parameters, displacement and angle, at the entrance of the wiggler should be the same as those at the exit. This imposes a symmetry on the field distribution along the beam trajectory, with a symmetry axis orthogonal to the straight section, lying on the orbit plane and passing through the wiggler center.

To reach the goal of having a very simple light source structure and a compensated magnetic field integral, a peculiar magnetic field pattern along the beam trajectory has been

adopted: a sharp vertical field peak (- 6 T, 14 cm f.w.h.m. Fig. 3) placed at the straight section center, compensated by two side tails (both decreasing from about + 1 T to zero in over 1 m of free straight section length).

The chosen field profile and symmetry, produce a single orbit bump in the horizontal plane, and the single "wiggle" gives rise to a single bright source spot in horizontal and vertical phase space.

The magnetic structure consists of a superconducting 6 T dipole, placed in a warm bore cryostat, and two (warm) side dipoles for field compensation (Fig. 4).

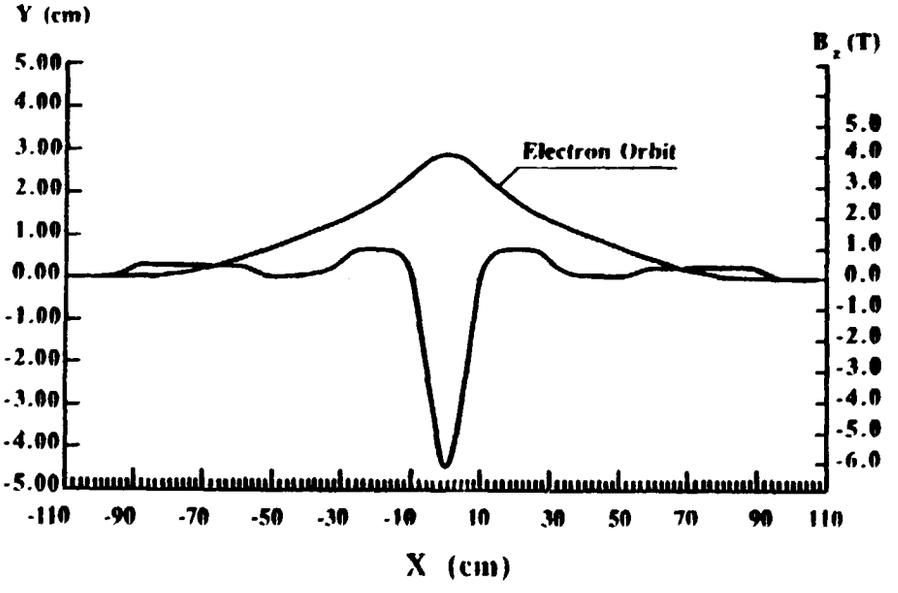

FIG. 3

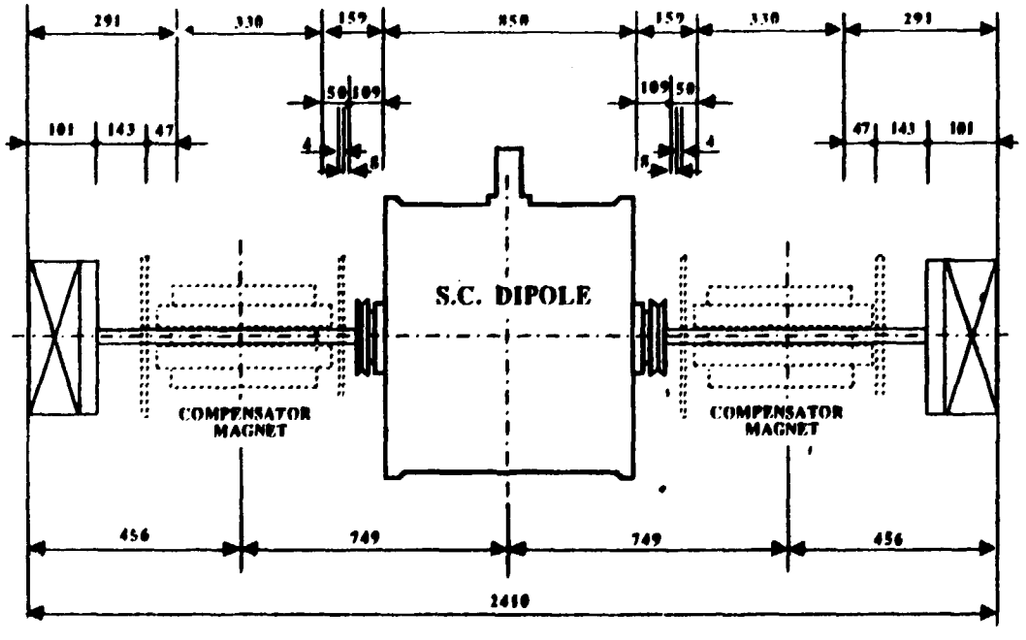

FIG. 4

The verification tests performed at the builder (Ansaldo Componenti), concern the superconducting dipole only. A brief description of the procedures and results are given in this preliminary report.

The s.c. dipole has 2 race-track NbTi coils, separated by a central stainless steel plate in which an elliptic bore has been milled (on axis) to accommodate the vacuum chamber. The coils are kept together by two iron yokes weighing 356 Kg together (Fig. 5). The magnet gap is 6 cm, in order to allow a beam stay clear of 3.2 cm in the above mentioned vacuum chamber. The chamber wall is surrounded by a small annular gap, under vacuum, containing the radiation heat shield consisting of 5 NRC-2 superinsulation layers. The maximum design operating current is 360 A. The computed static helium consumption of the cryostat is 5 l/h. The magnet is cooled with boiling helium, at 4.6°K and 1.4 atm., by a 1430S Koch liquefier/refrigerator connected to it through transfer lines.

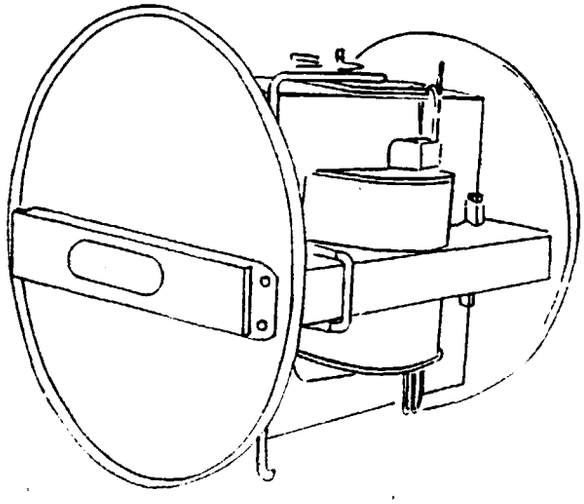

FIG. 5 - Cryomagnet's artistic view.

The verification tests deal with cryogenics (cool down and cryostat operation) magnet excitation (training and magnetization curve), magnetic measurement (field profile a. various excitation levels).

2. - COOL DOWN

The on line refrigerator of the Ansaldo workshop, where the tests have been carried out (Fig. 6), was not available, and the cryostat (capacity: 70 liters of liquid helium) was therefore simply filled first with liquid N_2 and then with He using dewars. During the first cool down, a safe cooling speed was adopted, of the order of 2 °K/hour. In the range from 300 to 80 °K the maximum Δt across the magnet has been 50 °K, measured through CLTS sensors. With reaching the liquid helium at its maximum level and after a thermalisation period, an average temperature of 50- 60 °K was measured at the radiation shields. The shields are cooled by boiling off the helium bath; the total evaporated volume (including the current leads cooling)

was about 5000 Nl/hour. The insulation vacuum was 2.10^{-6} Torr, maintained by a 100 l/hour diffusion pump.

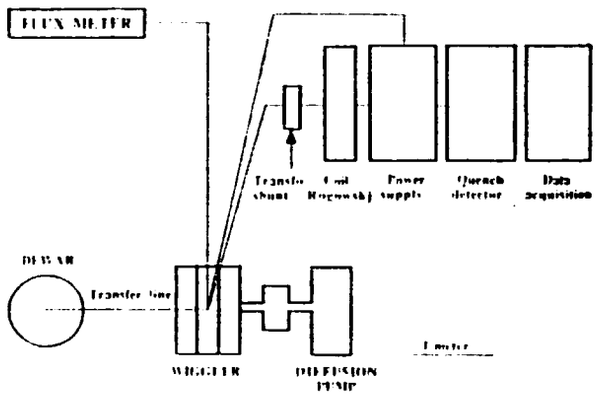

FIG. 6 - Wiggler testing area layout.

3. - MAGNET EXCITATION

The magnet mechanical structure is rather unusual if compared to that of a conventional superconducting dipole. This is due to the need of a large quasi-elliptic aperture (19x3.2 cm.) for the beam stay clear in Adone. In addition, as recalled above, the cryostat should have a warm bore, which means that the actual pole gap must accommodate also the bore vacuum insulation and this increases the transverse dimension of the magnetic yoke.

Fig. 7 shows the mechanical lay-out and it is clear that the large race track coils are supported by the magnet yoke only over a short length of the long side, and not at all at the curved heads. No reinforcing rings are allowed in order to avoid complicating the construction and enlarging the helium vessel transverse cross section. In spite of this mechanically unfavorable geometry, the magnet exceeded 6 Tesla after only few quenches all occurring above the 5.4 Tesla field level.

Fig. 8 shows the magnet training. The quenches were due to mechanical settlement of the coil and yoke under electromagnetic forces and not to conductor current limits. This has been proven by increasing the bath temperature from 4.2 K to that corresponding to a bath pressure of 1.41 bar (about 4.6 K) and finding no difference in the current values. At the above mentioned bath pressure the blowout disk behavior also has been tested by inducing a quench at the maximum magnet energy. The disk broke at 1.7 bar according to the calibration value.

Care was taken in finding the best ramping speed. A maximum ramp of 0.6 A/sec was adopted in the range from 0 to 290 A corresponding to a field of 5.560 Tesla; above this current value the ramp speed was reduced during training. The last quench occurred at 317.7 A corresponding to a field of 6.025 ± 0.003 Tesla. The maximum current level was attained by reducing the maximum ramp speed by a factor of ten. After reaching the 6 Tesla level no more quenches have been observed when repeating the ramp from zero to 6 Tesla. The magnet proved to be perfectly stable at every field level. The operating time was limited only by the helium availability.

The best de-energizing ramp speed has been found to be 1.2 A/sec max. The current leads, during the magnet excitation, were cooled by a helium flux of 2500 Nl/hour.

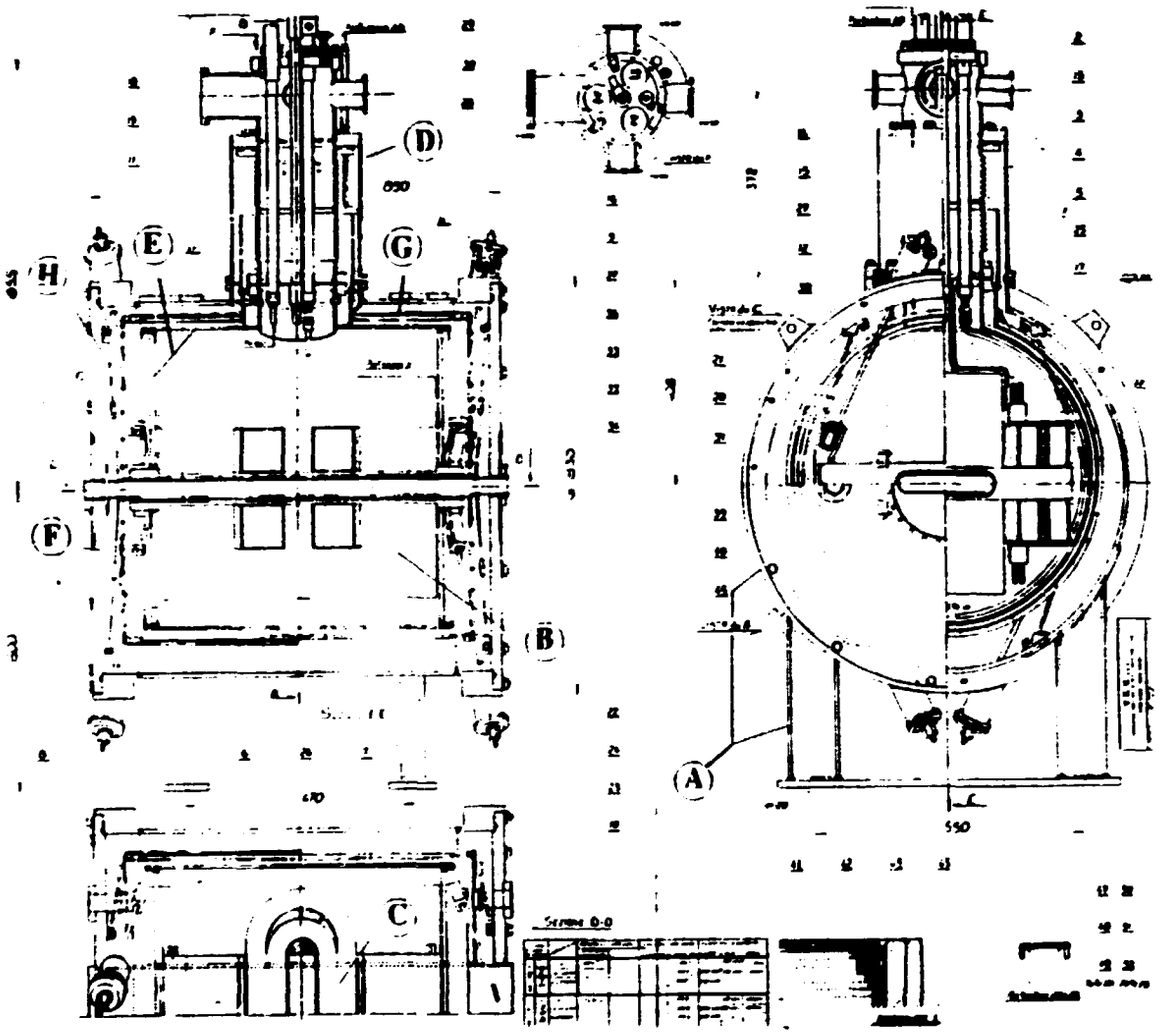

A: External vessel; B: Magnetic yokes; C: S.C. coils; D: Service turret;
E: Helium vessel; F: Flanges; G: Radiation screen; H: Suspension rods;

FIG. 7 - Transverse cross-section of the cryomagnet.

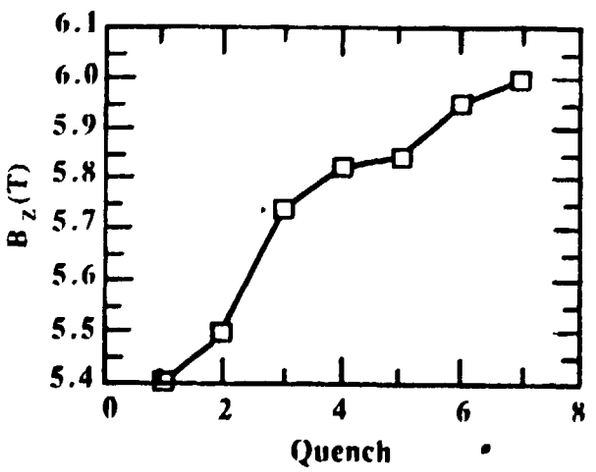

FIG. 8

4. - MAGNETIC FIELD PROFILES

The measurements have been made using an integrating magnetometer: a manually rotated small coil connected to an integrator made with very highly stabilized integrating circuits. The coil has a diameter of 5 mm and is 5 mm high. It has a measurement accuracy of 0.05 % of full scale over the three ranges 200 mT, 2 T, 20 T. The thermal drift, after two hours of running is less than 0.02 mT per minute. The instrument was built by Magnex (Abingdon, UK).

The flip coil was held in position and moved in steps along the wiggler symmetry axes using a mechanical actuator with an accuracy of better than 1/10 mm.

Field profiles have been measured at 5.0, 5.75, 6.0 Tesla. Fig. 9 shows the results and Fig. 10 shows the comparison with the output of the tridimensional computer codes Tosca and Magnus. The experimental data are in good agreement with the code previsions.

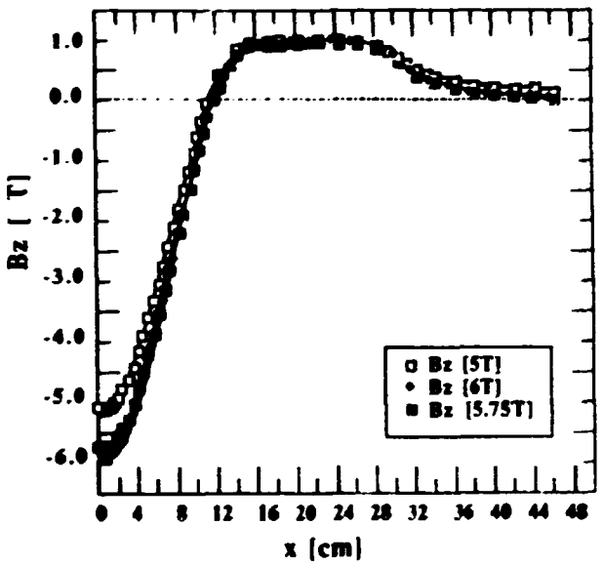

FIG. 9 - Wiggler S.CO.W. Bz (long).

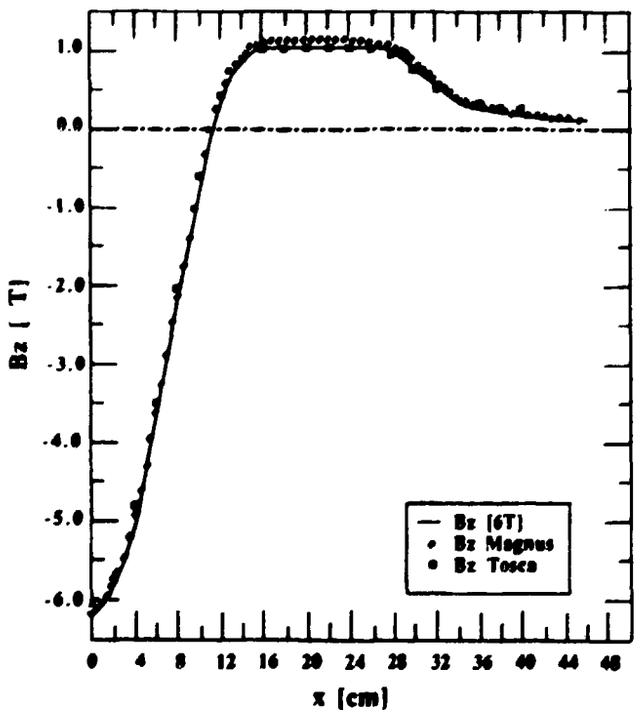

FIG. 10 - Wiggler S.CO.W. magnus and reality.

5 - PLANS FOR THE NEXT FUTURE

As mentioned above, the whole system consists of the superconducting dipole and two adjacent warm dipoles providing the field-integral compensation. The compensator magnets are "home made" and ready.

Magnetic measurements of the overall system are the most important task for the immediate future. In fact, to be compatible with the storage ring requirements, the field integral, along the beam trajectory (lieing on the symmetry plane of the wiggler) should vanish at all currents. Furthermore, the higher order terms of the field, integrated along the straight section where the wiggler is installed, should be kept below well defined limits.

To fulfill these specifications two kind of magnetic measurements will be carried out:
- point by point magnetic field map in the horizontal plane where the beam lies.
- field integral measurements along the magnet axis.

Hall probes will be used for the point by point maps, while a 3 meter long rotating coil, whose sensitivity was tested by measuring the earth magnetic field, (at Abingdon = 0.43 Gauss) will be used to measure the field integral and its integrated multipolar components. The field map measurements and the related equipment will be described in a paper to follow.

ACKNOWLEDGMENTS

The authors wish to thank Dr. M. Preger for calculating the intensity, the phase space distribution of the photon source and the effects of the s. c. wiggler on storage ring parameters, Dr. A. Savoia for many useful discussions during the system development phase, Dr. G. Modestino, Dr. F. Sgamma from LNF; last but not least Drs. G. Masullo, S. Parodi, R. Penco and M. Perrella, from Ansaldo Componenti S.p.A., for the support given during the verification tests.

REFERENCES

1) C.Sanelli: "Codice Poissson: applicazione al wiggler superconduttore" INFN, LNF - SCOW 1 - 15/12/1984
2) C.Sanelli: "Codice Poissson: programma Force -applicazione al wiggler superconduttore" - INFN, LNF - SCOW 2 - 22/1/1985
3) M.Preger, G. Turchetti: "Integrali di sincrotrone pre il wiggler s.c. a 3 poli" INFN, LNF - SCOW 4 - 8/3/1985
4) M.Preger, G. Turchetti: "Distribuzione nello spazio delle fasi radiali della luce di sincrotrone del wiggler superconduttore" - INFN, LNF - SCOW 5 - 11/3/1985
5) G.Modestino, M.Preger, G.Turchetti: "Wiggler superconduttore a polo singolo" INFN, LNF - SCOW 6 - 6/5/1985
6) A.Cattoni, G.Modestino: "Quench magnete wiggler superconduttore a polo singolo" INFN, LNF - SCOW 7 - 27/6/1985

7) G.Modestino, G.Turchetti: "Termine sestupolare per wiggler superconduttore a polo singolo" - INFN, LNF - SCOW 8 - 28/6/1985
8) A.Cattoni: "Termine sestupolare integrato: commenti" - INFN, LNF - SCOW 9 - 5/9/1985
9) C.Sanelli: "Wiggler superconduttore, nuova geometria" - INFN, LNF - SCOW 10 - 6/9/1985
10) F.Sgamma: "Wiggler superconduttore : deformazione del ferro dovuta alle forze prodotte dal campo magnetico" - INFN, LNF - SCOW 11 - 16/9/1985
11) A.Cattoni: "Sestupolo integrato: "Addendum a scow 9" - INFN, LNF - SCOW 12 - 11/9/1985
12) A.Cattoni, C.Sanelli: "Plateau sotto il polo e campo sulle bobine" - INFN, LNF - SCOW 13 - 8/10/1985
13) C.Sanelli: "Wiggler s.c. : campo disperso" - INFN, LNF - SCOW 14 - 19/12/1985
14) C.Sanelli: "Progetto dei magneti compensatori per S.CO.W." -INFN, LNF 85/64 (R) - 23/12/1985
15) G.Modestino, A.Savoia: "Linea di recupero dell'elio. Sovrappressione in caso di quench" - INFN, LNF - SCOW 15 - 9/5/1986
16) G.Modestino, M.Preger: "Effetti ottici del wiggler s.c. su Adone" - INFN, LNF - SCOW 16 - 12/5/1986
17) M.Perrella: "Progettazione costruttiva meccanico-criogenica bobine superconduttrici e criostato per magnete wiggler" - Ansaldo Componenti N. PMA/PRMA89R157 - 8/10/1986
18) C.Sanelli: "Prime misure sui magneti compensatori di SCOW" - INFN, LNF - SCOW 22 - 20/10/1988
19) A.Bixio, R.Marabotto, G.Spigo: "Verifiche magnetiche e meccaniche sul magnete wiggler" - Ansaldo Componenti N. PMA/PRMA88R095 - 26/10/1988
20) C.Sanelli: "Misura del campo residuo e caratterizzazione B-I dei magneti compensatori con magnetometro integratore E6000" - INFN, LNF - SCOW 23 - 28/10/1988
21) G.Masullo, S.Parodi: "Prove di vuoto, raffreddamento e di carica effettuate sul magnete wiggler" - Ansaldo Componenti N. PMA/PRMA89147 - 20/9/1989
22) M. Perrella: "Progettazione costruttiva meccanico-criogennica bobine superconduttrici e criostato per magnete wiggler" - Ansaldo Componenti N. PMA/PRMA89R157 - 8/10/1986.
23) A. Bixio, R. Marabotto, G. Spigo: Verifiche magnetiche e meccaniche sul magnete wiggler" - Ansaldo Componenti N. PMA/PRMA88R095 26/10/1988.
24) G. Masullo, S. Parodi: "Prove di vuoto, Raffreddamento e di carica effettuate sul magnete wiggler" - Ansaldo Componenti N. PMA/PRMA89147, 20/6/1989.